Quantum mechanical investigations of the $N(^4S)+O_2(X\,^3\Sigma_g^-)\rightarrow NO(X\,^2\Pi)+O(^3P)$ reaction

Renat A. Sultanov[a)]
Business Computer Research Laboratory, Saint Cloud State University, Saint Cloud, Minnesota 56301-4498

N. Balakrishnan[b)]
Department of Chemistry, University of Nevada Las Vegas, Las Vegas, Nevada 89154

(Received 16 December 2005; accepted 6 February 2006; published online 30 March 2006)

The reaction between energetic nitrogen atoms and oxygen molecules has received important attention in connection with nitric oxide chemistry in the lower thermosphere. We report time-independent quantum mechanical calculations of the $N(^4S)+O_2\rightarrow NO+O$ reaction employing the $X\,^2A'$ and $a\,^4A'$ electronic potential energy surfaces of Sayós *et al.* [J. Chem. Phys. **117**, 670 (2002)]. We confirm the production of highly vibrationally excited NO molecules, consistent with previous semiclassical and more recent time-dependent quantum wave packet studies. Calculations are carried out for total angular momentum quantum number $J=0$ and cross sections and rate coefficients are extracted using the J-shifting approximation. The results are in good agreement with available experimental and theoretical data. © *2006 American Institute of Physics*.
[DOI: 10.1063/1.2181143]

I. INTRODUCTION

Production of nitric oxide in collisions between energetic nitrogen atoms and oxygen molecules is a key process in atmospheric chemistry,

$$N(^4S)+O_2(X\,^3\Sigma_g^-)\rightarrow NO(X\,^2\Pi)+O(^3P). \quad (1)$$

The importance of the $N+O_2$ reaction in nitric oxide formation in the atmosphere was initially investigated by Zeldovich *et al.*[1] Reaction (1) together with the highly endoergic reaction,

$$O(^3P)+N_2(X\,^1\Sigma_g^+)\rightarrow NO(X\,^2\Pi)+N(^4S), \quad (2)$$

constitute the well known of Zeldovich mechanism.[1] Due to an activation energy of about 0.3 eV reaction (1) proceeds slow at room temperatures. However, the relatively large exoergicity of about 1.4 eV results in NO products with high vibrational-rotational (vj) excitation. Infrared emission from rovibrationally excited NO is considered to be an important mechanism for the night-time cooling of the thermosphere and much effort has been devoted to the determination of rovibrational level populations of NO resulting from (1).

Reaction (1) has received much attention in recent years[2–15] due to a longstanding discrepancy between observed levels of NO in the thermosphere and model predictions. Photochemical models were unable to predict the observed levels of NO in the thermosphere (peak NO density occurs near 105 km altitude) and reaction (1) involving nonthermal $N(^4S)$ atoms was suggested as an additional source of nitric oxide.[2] However, with improved calculation[15] of the energy distribution functions of the $N(^4S)$ atoms in the thermosphere and with updated photochemical models[16] the discrepancy has reduced to within 30%. Calculations by Sharma *et al.*[14] and Balakrishnan *et al.*[15] have shown that reaction (1) dominates NO production at altitudes above 120 km and the reaction between electronically excited $N(^2D)$ atoms and O_2 dominates at lower altitudes.

While the NO abundance issue appears to be more or less resolved,[16] quantitative determination of vibrational and rotational level populations of NO in the thermosphere still remains a major challenge. Because nitric oxide is one of the main radiating species in the thermosphere, accurate determination of the vibrational level population of NO is paramount to modeling the temperature variation in the thermosphere as well as understanding the composition, chemical structure, and the energy balance of the earth's atmosphere.

Reaction (1) has been the subject of a large number of experimental[17–26] and theoretical[27–43] investigations. The experimental studies have focused on two aspects: first, to evaluate thermal rate coefficients over a wide range of temperatures from 300 to 5000 K,[19,24,25] and second, to determine the rovibrational level populations of the $NO(v)$ products. The experimentally derived $NO(v)$ vibrational distribution shows a significant population of levels $v=0-7$. Early low resolution experimental results[17,20] demonstrated $NO(v)$ production up to $v\leqslant 7$. Subsequent higher resolution experiment[21] reported vibrational level-specific reaction rate coefficients for $v=2-7$. The first molecular beam measurement of NO vibrational level resolved cross section of reaction (1) was reported by Caledonia *et al.*[26] at a collision energy of 3.0 eV. The measured vibrational distribution shows an oscillatory behavior with peaks at $v=2$ and $v=4$. Similar oscillatory behavior was also observed in the room temperature measurement of $NO(v)$ product distributions by Winkler *et al.*[23] using resonant two-photon ionization techniques.

On the theoretical side, the presence of three heavy at-

a)Fax: 320-203-6074. Electronic mail: sultanov@bcrl.stcloudstate.edu
b)Fax: 702-895-4072. Electronic mail: naduvala@unlv.nevada.edu

oms makes accurate quantum mechanical calculations very challenging. Theoretical studies include quasiclassical trajectory (QCT) calculations,[28–33] quantum-classical methods,[34] variational transitional-state theory[31,34,41] (VTST), infinite-order-sudden approximation (IOSA) method, and quantum wave packet methods.[40] These calculations have used a variety of potential energy surfaces (PESs). The electronic structure calculations of the NO_2 system by Walch and Jaffe[27] have formed the basis of a number of potential energy surfaces for the $N+O_2$ reaction. More recently, improved calculations have been reported by Sayós *et al.*[41] and Caridade and Varandas.[42] The potential energy surface of Sayós *et al.*[41] has been used by Defazio *et al.*[40] who reported the first quantum mechanical calculations of NO rovibrational distributions from reaction (1). Caridade and Varandas[43] reported NO rovibrational distributions using QCT calculations on the PES of Varandas.[42] The results were found to be in close agreement with the QCT results of Ramachandran *et al.*[36] obtained using the potential surface of Duff *et al.*[30] and the $^4A'$ PES of Boss and Candler[33] which were based on the *ab initio* data of Walch and Jaffe.[27]

Here, we report the first three-dimensional time-independent quantum calculations of reaction (1). We use the NO_2 ground state $X\,^2A'$ and the first excited $a\,^4A'$ potential energy surfaces of Sayós *et al.*[41] for the calculations. The $X\,^2A'$ PES of Sayós *et al.*[41] has been used in the wave packet studies of Defazio *et al.*[40] For computational reasons, we restrict our calculations for total angular momentum $J=0$ and use the J-shifting approximation[44] to evaluate cross sections and rate coefficients. We report the results for initial state-selected probabilities, cumulative reaction probabilities, cross sections, rate coefficients, and final product distributions, and compare our findings to available experimental data, and to previous theoretical calculations.

The paper is organized as follows. In Sec. II we give a brief description of the methodology. The results of our calculations are presented in Sec. III and conclusions in Sec. IV.

II. METHOD

The reactive scattering calculations are carried out in hyperspherical coordinates using the ABC program[45] of Skouteris *et al.* The method involves simultaneous expansion of the wave function in Delves hyperspherical coordinates for all three arrangement channels of the A+BC system. Quantum reactive scattering boundary conditions are applied exactly to extract S-matrix elements $S^J_{v'j'k',vjk}$ for transitions from initial vibrational-rotational quantum numbers vj to final quantum numbers $v'j'$ for each value of the total angular momentum quantum number J. Initial rovibrational level resolved cross sections as functions of the incident kinetic energy E_{kin} are computed using the formula

$$\sigma_{vj}(E_{\mathrm{kin}}) = \frac{\pi}{k^2_{vj}(2j+1)} \sum_{J=0}^{\infty} (2J+1) P_{vjJ}(E_{\mathrm{kin}}), \tag{3}$$

where k_{vj} is the wave vector for the incident channel and $P^J_{vj}(E_{\mathrm{kin}})$ are the initial state-selected reaction probabilities given by

$$P_{vjJ}(E_{\mathrm{kin}}) = \sum_{v'j'k'k} |S^J_{v'j'k',vjk}(E_{\mathrm{kin}})|^2. \tag{4}$$

The angular momentum projection quantum numbers k and k' are restricted to values $0 \leqslant k \leqslant \min(J,j)$ and $0 \leqslant k' \leqslant \min(J,j')$. Initial state-selected rate constants are obtained by averaging the corresponding cross sections over a Boltzmann distribution of relative speeds of the colliding partners,

$$k_{vj}(T) = g\sqrt{\frac{8k_BT}{\pi\mu}} \int_0^{\infty} \frac{1}{(k_BT)^2} \sigma_{vj}(E_{\mathrm{kin}}) e^{-E_{\mathrm{kin}}/k_BT} E_{\mathrm{kin}} dE_{\mathrm{kin}}, \tag{5}$$

where g is the ratio between electronic partition function of the transition state and that of the reactant: $g=1/6$ for $X\,^2A'$ and $g=1/3$ for $a\,^4A'$ PESs, respectively, μ is the reduced mass of the atom-molecule system, T is the temperature, and k_B is the Boltzmann constant.

For an exact description of the dynamics, one needs to perform calculations for all contributing values of the total angular momentum quantum number J. Due to the presence of three heavy atoms and the large number of rovibrational levels for the diatomic fragments, explicit scattering calculations for $J>0$ are prohibitively expensive. Here, we use the simpler J-shifting approximation to obtain cross sections and rate coefficients. The J-shifting approximation was also adopted in the wave packet calculations reported by Defazio *et al.*[40] In general, the J-shifting approximation works well when the reaction proceeds through an energy barrier, as is the case for the present system. The J-shifting approach assumes that the reaction takes place through a transition state geometry and that the rotational energy $E^{\ddagger}_J$ of the triatomic species is not available to overcome the energy barrier. For the $X\,^2A'$ surface, the rotational constants $A^{\ddagger}$, $B^{\ddagger}$, and $C^{\ddagger}$ of the $[N-O-O]^{\ddagger}$ species are $A^{\ddagger}=2.246\ \mathrm{cm}^{-1}$, $B^{\ddagger}=0.330\ \mathrm{cm}^{-1}$, and $C^{\ddagger}=0.288\ \mathrm{cm}^{-1}$. For convenience, we use the symmetric-top expression for the rotational energy,

$$E^{\ddagger}_{JK} = \bar{B}^{\ddagger} J(J+1) + (A^{\ddagger} - \bar{B}^{\ddagger}) K^2, \tag{6}$$

where $\bar{B}^{\ddagger}=(B^{\ddagger}+C^{\ddagger})/2=0.309\ \mathrm{cm}^{-1}$. Similary, for the $^4A'$ surface, we obtain $A^{\ddagger}=1.903\ \mathrm{cm}^{-1}$ and $\bar{B}^{\ddagger}=0.352\ \mathrm{cm}^{-1}$. The values of the rotational constants for the $^2A'$ surface are in close agreement with those reported by Defazio *et al.* For the $^4A'$ surface Defazio *et al.* reported values $\bar{B}^{\ddagger}=0.340\ \mathrm{cm}^{-1}$ and $A^{\ddagger}-\bar{B}^{\ddagger}=1.860\ \mathrm{cm}^{-1}$ compared to $\bar{B}^{\ddagger}=0.352\ \mathrm{cm}^{-1}$ and $A^{\ddagger}-\bar{B}^{\ddagger}=1.550\ \mathrm{cm}^{-1}$ from our calculations. The difference is attributed to the difference in the $^4A'$ potential energy surfaces used: in the present study we use the $^4A'$ surface of Sayós *et al.*[41] while Defazio *et al.*[40] used the $^4A'$ surface of Duff *et al.*[30]

Cross sections for $J>0$ are obtained from the $J=0$ result by J shifting,

$$\sigma_{vj}(E_{\rm kin}) = \frac{\pi}{k_{vj}^2(2j+1)} \sum_{J=0}^{\infty} (2J+1) \sum_{K=-\min(j,J)}^{\min(j,J)} P_{vjJK}^{\ddagger}(E_{\rm kin}), \tag{7}$$

where the reaction probabilities $P_{vjJ}^{\ddagger}(E_{\rm kin})$ are calculated from the corresponding $J=0$ values according to

$$P_{vjJK}^{\ddagger}(E_{\rm kin}) = P_{vjJ=0}(E_{\rm kin} - E_{JK}^{\ddagger}). \tag{8}$$

Thermal rate coefficients are computed by Boltzmann averaging the cumulative reaction probability[46,47] (CRP),

$$k(T) = \frac{1}{2\pi\hbar Q_{\rm mol}(T)} \int_{-\infty}^{+\infty} e^{-E/k_BT} N(E) dE, \tag{9}$$

where E is the total energy and $Q_{\rm mol}(T)$ is the molecular reactant partition function obtained as the product of the electronic, vibrational, rotational, and translational partition functions: $Q_{\rm mol}(T)=Q_{\rm el}(T)Q_{\rm vib}(T)Q_{\rm rot}(T)Q_{\rm trans}(T)$, with $Q_{\rm el}(T)=1/g=6$ for the $^2A'$ surface and 3 for the $^4A'$ surface. The cumulative reaction probability $N(E)$ is given by

$$N_J(E) = \sum_{n_r,n_p} |S^J_{n_p \leftarrow n_r}(E)|^2, \tag{10}$$

where n_r and n_p refer to the collective quantum numbers of the reactant and products molecules.

When the J-shifting approximation is invoked, the final expression for the thermal rate coefficient becomes

$$k(T) = \frac{Q_{\rm rot}^{\ddagger}(T)}{2\pi\hbar Q_{\rm mol}(T)} \int_{-\infty}^{+\infty} e^{-E/k_BT} N_{J=0}(E) dE, \tag{11}$$

where $Q_{\rm rot}^{\ddagger}(T)$ is the rotational partition function of the transition state complex,

$$Q_{\rm rot}^{\ddagger}(T) = \sum_{J=0}^{\infty} (2J+1) \sum_{K=-J}^{J} e^{-E_{JK}^{\ddagger}/k_BT}. \tag{12}$$

If the nonadiabatic coupling between the $^2A'$ and $^4A'$ electronic states are neglected then the total rate coefficient is given by the sum of the rate coefficients evaluated separately on the two surfaces,

$$k(T) = k_{^2A'}(T) + k_{^4A'}(T). \tag{13}$$

Note that appropriate multiple surface coefficients for the two surfaces have been included in Eq. (9).

III. RESULTS

A. Convergence tests

Though the ABC program has been extensively used for a number of atom-diatom exchange reactions, most studies have focused on light atom transfer reactions such as $H+H_2$, $F+H_2$, $Cl+H_2$, and their isotopic counterparts. Recently, we have applied the program for reactions involving heavy atom transfer such as the F-atom transfer in the $Li+HF\rightarrow LiF+H$ and its reverse process[48,49] as well as reactions involving long-lived intermediate species such as the $H+O_2$ reaction.[50] For the present system, we have carried out extensive convergence tests with respect to different parameters that enter into the numerical solution of the Schrödinger equation. The results of convergence calculations will be presented first for several collision energies, ranging from the reaction threshold to about 2.0 eV. Although we carried out convergence tests for both PESs we only present the results for $^2A'$ PES, which has smaller barrier than $^4A'$ potential and consequently makes bigger contribution to cross sections at low energies.

TABLE I. Convergence of cumulative reaction probabilities $N_{J=0}(E)$ and initial state-selected probabilities $P_{0,1}(E)$ on the $^2A'$ potential with respect to maximum value of the hyperradius at which boundary conditions are applied. The results correspond to $e_{\rm max}=3.2$ eV, $j_{\rm max}=68$, and $N_{\rm max}=2133$.

E(eV)	$\rho_{\rm max}$	$N_{J=0}(E)$	$P_{0,1}(E)$
0.30	23.05	1.73(−05)[a]	7.26(−08)
	20.05	1.69(−05)	7.22(−08)
0.50	23.05	2.51	7.01(−02)
	20.05	2.42	7.05(−02)
0.70	23.05	9.62	3.87(−01)
	20.05	9.68	3.84(−01)
1.00	23.05	29.60	5.89(−01)
	20.05	29.70	5.88(−01)
1.20	23.05	48.50	6.80(−01)
	20.05	48.70	6.78(−01)

[a]Numbers in parentheses are powers of 10.

Convergence of the cumulative reaction probabilities and initial state-selected probabilities with respect to the hyperradius ρ are given in Table I. Our test calculations show that $\rho_{\rm max}=23.0a_0$ is adequate to obtain converged results.

Calculations were also done to test convergence with respect to the number of steps in the log-derivative method for radial integration along the hyperradius. We find that $\Delta\rho=0.05a_0$ is adequate for both potentials which led to $n_{\rm max}=460$ sectors for propagation along the hyperradius.

Tables II and III show the convergence tests with respect to the maximum value of the cutoff energy $e_{\rm max}$ and the maximum value of the rotational level $j_{\rm max}$, in any arrangement channel. In Table II we keep $j_{\rm max}=68$ and vary $e_{\rm max}$. It is seen that convergence within 5% is achieved for both CRPs, $N_{J=0}(E)$, and initial state-selected probabilities, $P_{0,1}(E)$ with $e_{\rm max}=2.7$ eV. Table III presents the convergence with respect to $j_{\rm max}$ for a fixed value of $e_{\rm max}=2.7$ eV. It is seen that $j_{\rm max}=90$ is adequate to obtain the converged results.

TABLE II. Convergence of CRPs and initial state-selected reaction probabilities with respect to $e_{\rm max}$ for a fixed value of $j_{\rm max}=68$ on the $^2A'$ PES. The maximum number of channels $N_{\rm max}$ is given in parentheses for each case.

	$e_{\rm max}=2.7$ eV ($N_{\rm max}=1793$)		$e_{\rm max}=3.2$ eV ($N_{\rm max}=2133$)	
E	$N_{J=0}(E)$	$P_{0,1}$(tot)	$N_{J=0}(E)$	$P_{0,1}$(tot)
0.30	1.47(−05)[a]	6.17(−08)	1.73(−05)	7.26(−08)
0.50	2.41	7.23(−02)	2.51	7.01(−02)
0.70	9.68	3.96(−01)	9.62	3.87(−01)
1.00	29.31	5.82(−01)	29.60	5.89(−01)
1.20	48.08	6.85(−01)	48.50	6.80(−01)

[a]Numbers in parentheses are powers of 10.

TABLE III. Convergence of CRPs and initial state-selected reaction probabilities with respect to j_{max} for a fixed value of e_{max}=2.7 eV on the $^2A'$ PES. The maximum number of channels N_{max} is given in parentheses for each case.

	j_{max}=68 (N_{max}=1793)		j_{max}=90 (N_{max}=2210)		j_{max}=98 (N_{max}=2329)	
E	$N_{J=0}(E)$	$P_{0,1}$(tot)	$N_{J=0}(E)$	$P_{0,1}$(tot)	$N_{J=0}(E)$	$P_{0,1}$(tot)
0.30	1.47(−05)[a]	6.17(−08)	1.78(−05)	7.54(−08)	1.5(−05)	6.30(−08)
0.50	2.41	7.23(−02)	2.30	6.34(−02)	2.35	6.80(−02)
0.70	9.68	3.96(−01)	9.66	3.92(−01)	9.67	4.00(−01)
1.00	29.31	5.8(−01)	29.52	5.87(−01)	29.51	5.8(−01)
1.20	48.08	6.85(−01)	48.89	6.85(−01)	49.06	6.82(−01)
1.60	⋯	⋯	96.66	8.21(−01)	96.72	8.29(−01)
2.00	⋯	⋯	160.65	8.14(−01)	161.74	8.21(−01)

[a]Numbers in parentheses are powers of 10.

Based on these convergence tests, we use e_{max}=2.7 eV and j_{max}=90 in our production calculations. This led to a total of 2210 rovibrational basis functions in the calculations.

B. Cross sections, rate coefficients, and product NO(v') distribution

In Fig. 1 we present the initial state-selected probabilities $P_{v=0,j=1,J=0}$ computed on the two potentials as functions of the incident kinetic energy. The results on the $^2A'$ surface are essentially negligible for energies below 0.3 eV, consistent with an energy barrier of about 0.3 eV. Our results are in good agreement with the time-dependent wave packet calculations of Defazio *et al.*[40] for energies less than 1.0 eV. Comparison with Fig. 1(b) of Defazio *et al.*[40] shows that the present results are about 15% higher for energies above 1.0 eV. The discrepancies at higher energies may be attributed to the different numerical procedures, convergence criteria, and basis set sizes adopted in the two calculations. As Table III illustrates, the present results are converged to better than 5% for energies above 1.0 eV. The results on the $^4A'$ surface show a threshold of 0.62 eV which is the same as the wave packet calculations of Defazio *et al.* who employed the $^4A'$ surface of Duff *et al.*[30] Our results are somewhat smaller than those of Defazio *et al.* for energies lower than 1.0 eV. This is attributed to an artificial barrier in the entrance channel of the $^4A'$ surface of Sayós *et al.*[41] used in the present study. However, this does not affect the final rate coefficients because contributions from the $^2A'$ surface dominate for energies lower than 1.0 eV. At higher energies quantitative agreement is obtained with the results of the wave packet calculations.[40]

In Fig. 2 we compare the J-shifted cross sections on the $^2A'$ surface with the corresponding results of Defazio *et al.*[40] as well as the mixed quantum classical results of Balakrishnan and Dalgarno.[35] The agreement between the present results and those of Defazio *et al.* is excellent for energies up to 1.5 eV. As in the case of reaction probabilities, the present results are slightly higher for energies above 1.5 eV. The mixed quantum-classical (QC) results are obtained using an earlier $^2A'$ potential of Sayós *et al.*[34] It is seen that the QC results are in reasonable agreement with the J-shifted quantum results, implying that the J-shifiting approximation is reliable for the present system. Comparison of the behavior of the cross sections from the quantum and QC calculations near the threshold shows that quantum effects are not very significant in the dynamics of the reaction.

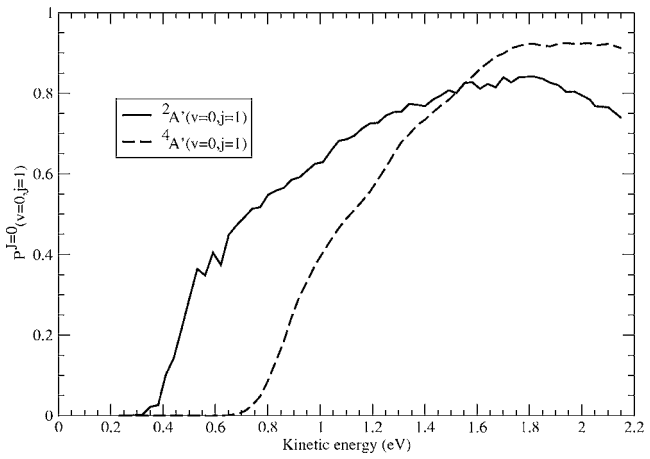

FIG. 1. Initial state-selected probabilities $P^J_{vj}(E_{kin})$ for the $N+O_2(v=0,j=1)$ reaction occurring on the $X\,^2A'$ and $a\,^4A'$ PESs as functions of the collision energy.

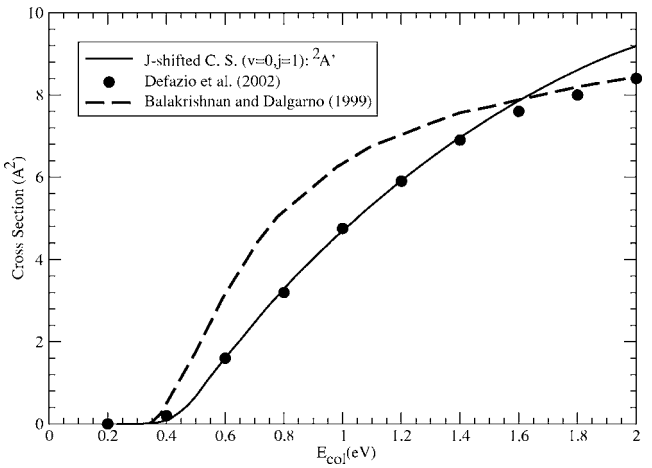

FIG. 2. Initial state-selected cross section $\sigma_{vj}(E_{kin})$ for the $N+O_2(v=0,j=1)$ reaction occurring on the $X\,^2A'$ PES as a function of the collision energy together with the time-dependent quantum results of Defazio *et al.* (Ref. 40) and the quantum-classical results of Balakrishnan and Dalgarno (Ref. 35).

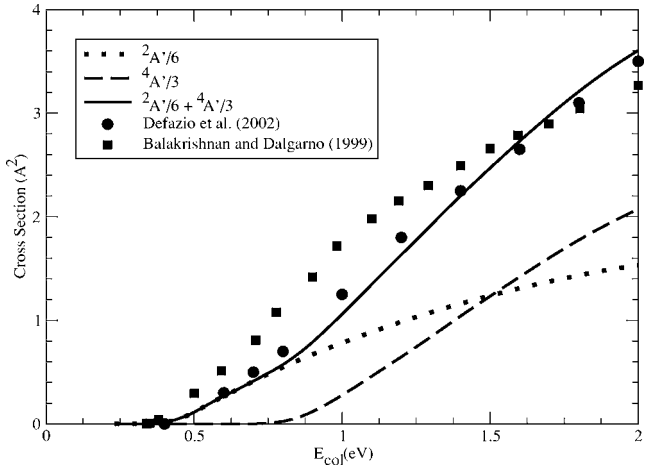

FIG. 3. Initial state-selected cross sections $\sigma_{vj}(E_{\mathrm{kin}})$ including the electronic degeneracies for the $N+O_2(v=0,j=1)$ reaction occurring on the $X\,^2A'$ and $a\,^4A'$ PESs as functions of the collision energy together with the time-dependent quantum results of Defazio *et al.* (Ref. 40) and the quantum-classical results of Balakrishnan and Dalgarno (Ref. 35).

Figure 3 compares the electronic degeneracy averaged cross sections on the two potential surfaces from the present study and those of Defazio *et al.* The QC results of Balakrishnan and Dalgarno[35] are also included for comparison. It is seen that the quantum results agree with each other and are also in reasonable accord with the QC results. The quantum results are consistently lower than the QC results for energies below 1.5 eV. We believe that this is, due in part, to the *J*-shifting approximation. We also note that the PESs used in the present study are different from the ones employed in the QC calculations. The slight underestimation of the total degeneracy averaged cross sections from the present calculations compared with that of Defazio *et al.* in the energy range of 0.8–1.2 eV is due to the smaller probabilities obtained on the $^4A'$ potential of Sayós *et al.*[41] used in the present study.

Initial sate-selected rate coefficients k_{01} evaluated on the two PESs are shown in Fig. 4. It is seen that for temperatures lower than 2000 K contribution from the $^2A'$ PES dominates. Numerical values of the rate coefficients are given in Table IV in the temperature range of 200–2000 K.

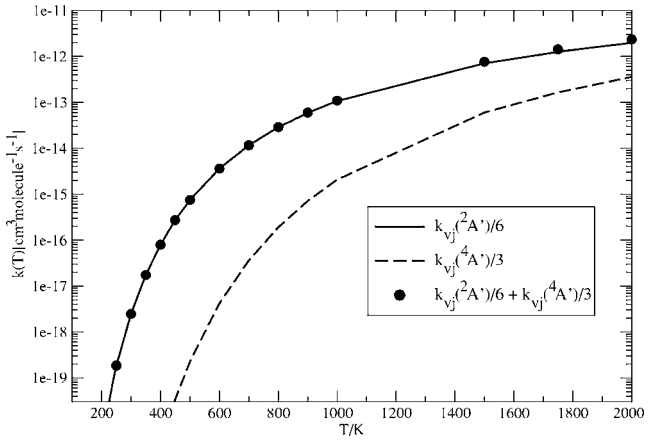

FIG. 4. Initial state-selected rate coefficients $k_{v=0,j=1}(T)$ including the electronic degeneracies for the $N+O_2(v=0,j=1)$ reaction occurring on the $X\,^2A'$ and $a\,^4A'$ PESs as functions of the temperature.

TABLE IV. Initial state-selected rate coefficients $k_{v=0,j=1}(^2A')$, $k_{v=0,j=1}(^2A')$ and their sum (cm^3 $molecule^{-1}$ s^{-1}) for reaction (1) as functions of the temperature.

T (K)	$k_{v=0,j=1}(^2A')$	$k_{v=0,j=1}(^4A')$	$k_{v=0,j=1}(^2A')+k_{v=0,j=1}(^4A')$
200.00	4.57(−21)[a]	3.54(−29)	4.57(−21)
250.00	1.85(−19)	3.29(−26)	1.85(−19)
300.00	2.48(−18)	4.63(−24)	2.48(−18)
350.00	1.73(−17)	1.88(−22)	1.73(−17)
400.00	7.96(−17)	3.38(−21)	7.96(−17)
450.00	2.72(−16)	3.38(−20)	2.72(−16)
500.00	7.47(−16)	2.25(−19)	7.47(−16)
600.00	3.60(−15)	4.18(−18)	3.60(−15)
700.00	1.16(−14)	3.61(−17)	1.16(−14)
800.00	2.87(−14)	1.90(−16)	2.89(−14)
900.00	5.92(−14)	7.10(−16)	5.99(−14)
1000.0	1.07(−13)	2.08(−15)	1.09(−13)
1500.0	7.07(−13)	6.00(−14)	7.67(−13)
1750.0	1.26(−12)	1.65(−13)	1.43(−12)
2000.0	1.98(−12)	3.58(−13)	2.34(−12)

[a]Numbers in parentheses are powers of 10.

There is much interest in the vibrational distributions of the NO molecule resulting from the reaction. Nitric oxide is one of the main sources of infrared emission in the upper atmosphere through its fundamental and first overtone bands and determination of vibrational level populations of NO is key to accurately modeling the chemical composition and thermal structure of the upper atmosphere. Most experimental studies[21,23] have focused on the product branching ratio,

$$D_{v'}(T)=\frac{k_{v'}(T)}{\Sigma_{v'}k_{v'}(T)}, \tag{14}$$

where $k_{v'}(T)$ are the rate coefficients for the production of $NO(v')$ from a thermal population of rovibrational levels of the O_2 molecules. Since the present calculations are restricted to $v=0$, $j=1$ level of the O_2 molecule, we present the quantity

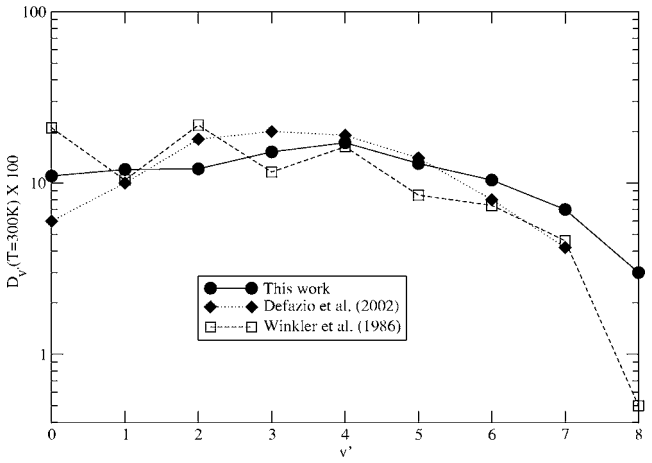

FIG. 5. Vibrational distribution $D_{v'}(T)$ of $NO(v')$ products at 300 K.

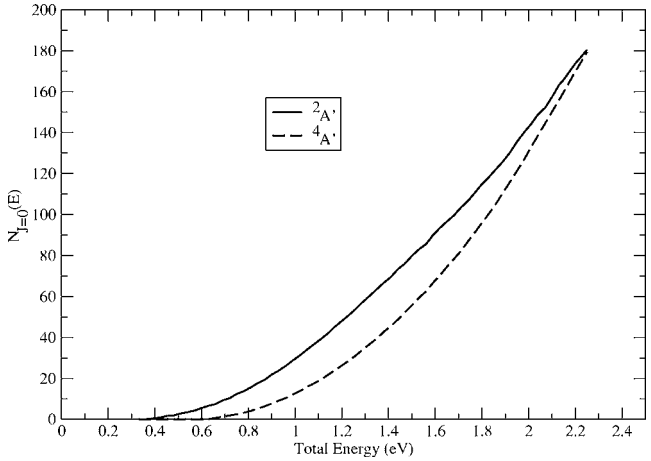

FIG. 6. Cumulative reaction probabilities for the $N+O_2$ reaction occurring on the $X\,^2A'$ and $a\,^4A'$ PESs.

$$D_{v'}(T) = \frac{k_{v=0,j=1,v'}(T)}{\Sigma_{v'=0,8} k_{v=0,j=1,v'}(T)}, \tag{15}$$

where $k_{v=0,j=1,v'}(T)$ are the state-to-state rate coefficients evaluated using an expression similar to that of Eq. (5). Our results for $D_{v'}$ at 300 K are presented in Fig. 5 along with the experimental data of Winkler *et al.*[23] and the quantum results of Defazio *et al.*[40] It is seen that our results peak at $v'=4$ and decrease rapidly with increase in v'. The results are in close agreement with the quantum results of Defazio *et al.* which show comparable values for $v'=2-4$ with a slight preference for $v'=3$. The experimental data of Winkler *et al.* are somewhat oscillatory with a preference for even v' levels. A direct comparison with the experimental data or the quantum results of Defazio *et al.* is not possible because our calculations do not include contributions from $j>1$ levels of the O_2 molecule. Our results are also not directly comparable to the crossed molecular beam measurements of Caledonia *et al.*[26] because the experimental results were obtained at a center-of-mass collision energy of 3.0 eV. This also applies to the QCT results of Ramachandran *et al.*[36] and Caridade and Varandas[43] which were obtained at an energy of 3.0 eV to model the experimental results of Caledonia *et al.* However, these theoretical studies were not successful in reproducing the measured results of Caledonia *et al.*

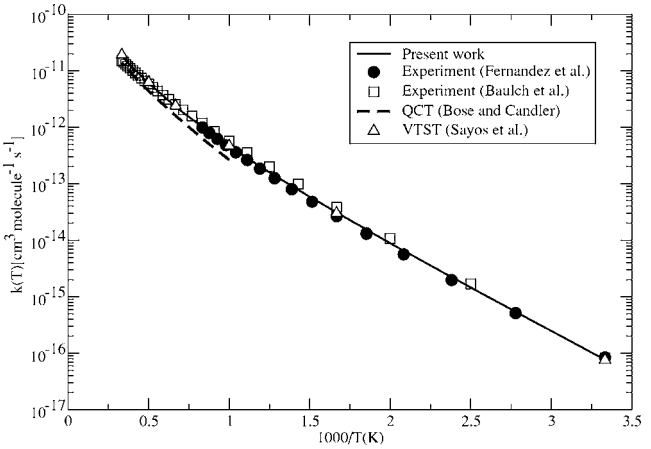

FIG. 7. Comparison of the thermal rate coefficients for the $N+O_2$ reaction with the experimental and theoretical results as functions of the temperature: solid curve—present results; filled circles—experimental data of Fernandez *et al.* (Ref. 25); open squares—experimental data of Baulch *et al.* (Ref. 24); dashed curve—QCT results of Bose and Candler (Ref. 33); open triangles—VTST results of Sayós *et al.* (Ref. 41).

Figure 6 shows $J=0$ CRPs computed on the $^2A'$ and $^4A'$ PESs. Thermal rate coefficients were evaluated using the cumulative reaction probabilities, by invoking the J-shifting approximation. In Fig. 7 we compare the thermal rate coefficients from the present studies with the experimental data of Baulch *et al.*[24] and Fernandez *et al.*,[25] the QCT results of Bose and Candler,[33] and the VTST results of Sayós *et al.*[41] The quoted error bars for the experimental data of Baulch *et al.*[24] are $\Delta \log k = \pm 0.12$ for $300 \leqslant T \leqslant 1000$ K and $\Delta \log k = \pm 0.30$ for $1000 < T \leqslant 3000$ K. It is seen that our results are in excellent agreement with the experiments and the QCT and VTST results demonstrating that the J-shifting approximation may be used for accurate determination of thermal rate coefficient for the present system. However, a

TABLE V. Thermal rate coefficients $k_{NO_2}(T)$ (cm^3 molecule^{-1} s^{-1}) on the two PESs for reaction (1) together with available experimental and theoretical results.

T (K)	$k^{2}{}_{A'}$	$k^{4}{}_{A'}$	$k(T)=k^{2}{}_{A'}+k^{4}{}_{A'}$	Expt.[a]	Expt.[b]	Defazio *et al.*[c]
300.00	6.00(−17)[d]	8.04(−21)	6.00(−17)	8.42(−17)	8.31(−17)	3.53(−17)
350.00	3.42(−16)	1.67(−19)	3.42(−16)	3.96(−16)	4.60(−16)	
400.00	1.26(−15)	1.68(−18)	1.26(−15)	1.32(−15)	1.69(−15)	
450.00	3.48(−15)	1.03(−17)	3.49(−15)	3.45(−15)	4.71(−15)	
500.00	7.94(−15)	4.46(−17)	7.98(−15)	7.64(−15)	1.08(−14)	
600.00	2.80(−14)	4.14(−16)	2.84(−14)	2.65(−14)	3.87(−14)	1.55(−14)
700.00	7.04(−14)	2.09(−15)	7.25(−14)	6.79(−14)	9.83(−14)	
800.00	1.43(−13)	7.21(−15)	1.50(−13)	1.43(−13)	2.01(−13)	
900.00	2.53(−13)	1.92(−14)	2.72(−13)	2.62(−13)	3.57(−13)	
1000.0	4.03(−13)	4.24(−14)	4.45(−13)	4.37(−13)	5.70(−13)	2.39(−13)
1500.0	1.80(−12)	5.06(−13)	2.31(−12)	2.45(−12)	2.54(−12)	1.22(−12)
2000.0	4.13(−12)	1.91(−12)	6.04(−12)	6.97(−12)	5.85(−12)	3.23(−12)
2500.0	7.11(−12)	4.40(−12)	1.15(−11)	1.45(−11)	1.01(−11)	
3000.0	1.04(−11)	7.81(−12)	1.82(−11)	2.55(−11)	1.51(−11)	9.88(−12)

[a]Reference 25.
[b]Reference 24.
[c]Reference 40.
[d]Numbers in parentheses are powers of 10.

rigorous determination of the validity of the *J*-shifting approximation would require exact quantum calculations for higher values of *J* which are beyond the scope of the present study, and indeed very challenging for the present system. Numerical values of the rate coefficients in the temperature range of 300–3000 K are given in Table V along with the experimental data of Baulch *et al.* and Fernandez *et al.* as well as the time-dependent quantum results of Defazio *et al.*[40] We believe that the significant underestimation of the theoretical results of Defazio *et al.* is due to the restricted number of initial v and j levels included in the thermal population as well as the approximations $k_{vj}\approx k_{v11}$ for $j>11$. No such restriction is imposed on the present calculations as the thermal rate coefficients are evaluated using the full $J=0$ cumulative reaction probabilities.

IV. CONCLUSION

In this paper, we have presented the first detailed time-independent quantum calculations of the $N+O_2$ reaction on the two lowest adiabatic potential surfaces. The presence of three heavy atoms and the large exoergicity of the reaction that populates many high lying NO rovibrational levels make quantum calculations extremely challenging. Even though the results reported here are restricted to total angular momentum quantum number $J=0$, the calculations are computer intensive. However, we have demonstrated that the *J*-shifting approximation can be used to reliably extract cross sections and rate coefficients. Vibrational populations of NO obtained from our calculations compare favorably with the time-dependent quantum results of Defazio *et al.*[40] While we obtain excellent agreement with experiment for thermal rate coefficients, there still exists some discrepancy with the experimental results for product vibrational distribution. Whether the differences are due to the *J*-shifting approximation or inaccuracies in the potential energy surfaces employed in the calculations is not clear. While quantum calculations involving higher values of *J* are clearly desirable, such calculations are formidable for the present system and are beyond the scope of the present study.

ACKNOWLEDGMENTS

This work was supported in part by the National Science Foundation through Grant No. ATM-0205199. Acknowledgment is also made to the Donors of the American Chemical Society Petroleum Research Fund for partial support of this research.

[1] J. B. Zeldovich, P. J. Sadovnikov, and D. A. Frank-Kamenetski, *Nitrogen Oxidation under Combustion* (Academy of Sciences, Moscow, 1947), p. 64.
[2] S. Solomon, Planet. Space Sci. **31**, 135 (1983).
[3] D. E. Siskind, C. A. Barth, and D. D. Cleary, J. Geophys. Res. **95**, 4311 (1990).
[4] J.-C. Gérard, V. I. Shematovich, and D. V. Bisikalo, Geophys. Res. Lett. **18**, 1695 (1991).
[5] O. Lie-Svendsen, M. H. Rees, K. Stamnes, and E. C. Whipple, Planet. Space Sci. **39**, 929 (1991).
[6] R. D. Sharma, Y. Sun, and A. Dalgarno, Geophys. Res. Lett. **20**, 2043 (1993).
[7] R. D. Sharma, V. A. Kharchenko, Y. Sun, and A. Dalgarno, J. Geophys. Res. **101**, 275 (1996).
[8] R. D. Sharma, H. Dothe, F. von Esse, V. A. Kharchenko, Y. Sun, and A. Dalgarno, J. Geophys. Res. **101**, 19707 (1996).
[9] H. Dothe, R. D. Sharma, and J. W. Duff, Geophys. Res. Lett. **24**, 3233 (1997).
[10] J.-C. Gérard, D. V. Bisikalo, V. I. Shematovich, and J. W. Duff, J. Geophys. Res. **102**, 285 (1997).
[11] P. K. Swaminathan, D. F. Strobel, D. G. Kupperman *et al.*, J. Geophys. Res. **103**, 11,579 (1998).
[12] V. Kharchenko, N. Balakrishnan, and A. Dalgarno, J. Atmos. Sol.-Terr. Phys. **60**, 95 (1998).
[13] N. Balakrishnan, V. Kharchenko, and A. Dalgarno, J. Chem. Phys. **108**, 943 (1998).
[14] R. D. Sharma, H. Dothe, and J. W. Duff, J. Geophys. Res. **103**, 14753 (1998).
[15] N. Balakrishnan, E. Sergueeva, V. Kharchenko, and A. Dalgarno, J. Geophys. Res. **105**, 18549 (2000).
[16] P. K. Swaminathan, D. F. Strobel, L. Acton, and L. J. Paxton, Phys. Chem. Earth (C) **26**, 533 (2001).
[17] F. Hushfar, J. W. Rogers, and A. T. Stair, Jr., Appl. Opt. **10**, 1843 (1971).
[18] C. T. Bowman, Combust. Sci. Technol. **3**, 37 (1971).
[19] D. L. Baulch, D. D. Drysdale, and D. G. Haine, *Evaluated Kinetic Data for High Temperature Reactions* (Butterworths, London, 1973), Vol. 2.
[20] M. E. Whitson, Jr., L. A. Darnton, and R. J. McNeal, Chem. Phys. Lett. **41**, 552 (1976).
[21] A. Rahbee and J. J. Gibson, J. Chem. Phys. **74**, 5143 (1981).
[22] R. R. Herm, B. J. Sullivan, and M. E. Whitson, Jr., J. Chem. Phys. **79**, 2221 (1983).
[23] I. C. Winkler, R. A. Stachnik, J. I. Steinfeld, and S. M. Miller, J. Chem. Phys. **85**, 890 (1986).
[24] D. L. Baulch, C. J. Cobos, R. A. Cox, J. Phys. Chem. Ref. Data **23**, 847 (1994).
[25] A. Fernandez, A. Goumri, and A. Fontijn, J. Phys. Chem. A **102**, 168 (1998).
[26] G. E. Caledonia, R. H. Krech, D. B. Oakes, S. J. Lipson, and W. A. M. Blumberg, J. Geophys. Res. **105**, 12833 (2000).
[27] S. P. Walch and R. L. Jaffe, J. Chem. Phys. **86**, 6946 (1987).
[28] M. Gilibert, A. Aguilar, M. Gonzáles, and R. Sayós, Chem. Phys. **172**, 99 (1993); **178**, 287 (1993).
[29] R. Sayós, A. Aguilar, M. Gilibert, and M. Gonzáles, J. Chem. Soc., Faraday Trans. **89**, 3223 (1993).
[30] J. W. Duff, F. Bien, and D. E. Paulsen, Geophys. Res. Lett. **21**, 2043 (1994).
[31] G. S. Valli, R. Orrú, E. Clementi, A. Laganá, and S. Crocchianti, J. Chem. Phys. **102**, 2825 (1995).
[32] M. Gilibert, X. Gimenez, M. Gonzáles, R. Sayós, and A. Aguilar, Chem. Phys. **191**, 1 (1995).
[33] D. Bose and G. V. Candler, J. Chem. Phys. **107**, 6136 (1997).
[34] R. Sayós, J. Hijazo, M. Gilibert, and M. González, Chem. Phys. Lett. **284**, 101 (1998).
[35] N. Balakrishnan and A. Dalgarno, Chem. Phys. Lett. **302**, 485 (1999).
[36] B. Ramachandran, N. Balakrishnan, and A. Dalgarno, Chem. Phys. Lett. **332**, 562 (2000).
[37] R. Sayós, C. Olivia, and M. Gonzáles, J. Chem. Phys. **115**, 1287 (2001).
[38] P. Defazio, C. Petrongolo, S. K. Gray, and C. Olivia, J. Chem. Phys. **115**, 3208 (2001).
[39] M. Gonzales, C. Olivia, and R. Sayós, J. Chem. Phys. **117**, 680 (2002).
[40] P. Defazio, C. Petrongolo, C. Olivia, M. Gonzales, and R. Sayós, J. Chem. Phys. **117**, 3647 (2002).
[41] R. Sayós, C. Olivia, and M. Gonzáles, J. Chem. Phys. **117**, 670 (2002).
[42] A. J. C. Varandas, J. Chem. Phys. **119**, 2596 (2003).
[43] P. J. S. B. Caridade and A. J. C. Varandas, J. Phys. Chem. A **108**, 3556 (2004).
[44] J. M. Bowman, J. Chem. Phys. **95**, 4960 (1991).
[45] D. Skouteris, J. F. Castillo, and D. E. Manolopoulos, Comput. Phys. Commun. **133**, 128 (2000).
[46] W. H. Miller, J. Chem. Phys. **62**, 1899 (1975).
[47] W. H. Miller, S. D. Schwartz, and J. W. Tromp, J. Chem. Phys. **79**, 4889 (1983).
[48] P. F. Weck and N. Balakrishnan, J. Chem. Phys. **122**, 234310 (2005).
[49] P. F. Weck and N. Balakrishnan, J. Chem. Phys. **122**, 154309 (2005).
[50] R. A. Sultanov and N. Balakrishnan, J. Phys. Chem. A **108**, 8759 (2004).